PROPOSAL FOR AN EXPERIMENT

PAC Date	EXP#
DECEMBER 2021	**E843_21**

Title: Study of 68Ni by neutron adding and removing reactions

Spokesperson: Koyama Shumpei
Affiliation: GANIL,

Phone:	Fax:	Email: shumpei.koyama@ganil.fr

Backup Spokesperson: Sorlin Olivier
Affiliation: GANIL

Phone:	Fax:	Email: Sorlin@ganil.fr

Backup Spokesperson: Mengoni Daniele
Affiliation: University and INFN, Padova

Phone:	Fax:	Email: Daniele.mengoni@pd.infn.it

GANIL contact person : Clement Emmanuel (clement@ganil.fr)

Abstract:

We propose to investigate the shell structure of ^{68}Ni via neutron adding and removal reactions. By combining the vacancy and occupancy of each neutron orbital in ^{68}Ni from the transfer reactions, the neutron Fermi surface at N=40 is studied. We plan to re-measure the $d_{5/2}$ single particle state(s) in ^{69}Ni via the (d,p) reaction to confirm its excitation energy and spin-parity with slow-downed beam at 18 MeV/u. The complimentary measurement of the neutron removing (p,d) and (d,t) reactions will be also performed to investigate the neutron occupancies of ^{68}Ni. These reactions also enable us to access the spin-orbit splitting of 2p, 1f, and 1g orbitals in ^{68}Ni. The experiment will be performed with MUGAST@LISE setup including EXOGAM2 and newly developing Zero Degree Detection system.

COLLABORATION

Assié Marlène (IPN)
Balogh Matus (INFN-LNL)
Beaumel Didier (IPN Orsay)
Blumenfeld Yorick (IPN Orsay)
Bottoni Simone (Università degli Studi di Milano and INFN)
Brugnara Daniele (Legnaro National Laboratories)
Caceres Lucia (GANIL)
Clement Emmanuel (CNRS)
De Angelis Giacomo (INFN - Laboratori Nazionali Legnaro)
De France Gilles (GANIL)
De Séréville Nicolas (IJCLab)
Diget Christian (University of York)
Fernandez Dominguez Beatriz (USC)
Galtarossa Franco (Università di Padova and INFN Laboratori Nazionali di Legnaro) (PDF)
Goasduff Alain (LNL, INFN)
Gottardo Andrea (INFN - Laboratori Nazionali di Legnaro, LEGNARO)
Ha Jeongsu (Università degli Studi di Padova and INFN-Padova) (PDF)
Hammache Fairouz (IIJCLab)
Harrouz Djamila Sarah (IJCLab) (S)
Kamalou Omar (GANIL)
LEMASSON Antoine (GANIL)
Laird Alison (University of York)
Lenzi Silvia (University of Padova and INFN)
Leoni Silvia (University of Milano and INFN)
Mengoni Daniele (University and INFN, Padova)
Moukaddam Mohamad (University of Strasbourg, IPHC)
Napoli Daniel R. (INFN - LNL)
Niikura Megumi (The University of Tokyo)
Pellumaj Julgen (University of Ferrara Italy, INFN-LNL) (S)
Pérez Vidal Rosa María (INFN-LNL) (PDF)
Rezynkina

Kseniia (ONFN-Padova) (PDF)
Roger Thomas (GANIL)
Sedlak Matus (LNL INFN)
Sorlin Olivier (GANIL)
Stefan Gheorghe Iulian (IPN Orsay)
Stodel Christelle (GANIL)
Suzuki Daisuke (RIKEN Nishina Center)
THOMAS Jean-Charles (GANIL)
Valiente Dobon Jose Javier (LNL-INFN)
Zago Luca (INFN Legnaro National Laboratories) (S)
Zanon Irene (Laboratori Nazionali di Legnaro - INFN) (S)
Zhang Guangxin (Padova-Infn) (PDF)

EXPERIMENTAL DEVICES REQUIRED

BEAM LINES- D6 LISE Without Wien Filter
DETECTION SYSTEMS- CATS
DETECTION SYSTEMS- EXOGAM
DETECTION SYSTEMS- MUGAST
DETECTION SYSTEMS- MUST2
Additional information: Zero Degree Detection system for the end of beam line HPGe Clover for isomer measurement

EXPERIMENTAL SET UP

Reaction Targets: CD2 (0.5 mg/cm2), CH2 (5 mg/cm2)
Data Acquisition: GANIL

Already performed: YES
Experiment number(s) that used the same (or similar) experimental setup: E738 and E755
Differences or improvements: MUST2 was used for (p,d) measurement with Ionizing chamber at the zero degrees. MUGAST setup for (d,p) and (p,d) will be used with newly developing Zero Degree Detection system. EXOGAM2 will be also used for gamma-ray detection.
Similar setups: YES
Details: MUGAST@LISE setup planned in 2023 (spokespersons S. Bottoni and F. Galtarossa). The setup is common for these experiments except for beams.

BEAM REQUEST

Beam	Ion(s)	Energy (MeV/u)	Intensity on target (pps)	Purity (%)	Beam extension (ns)
LISE	68Ni	18	40000	80	
Stable	70Zn	62			

LISE Production Beam :

Material	Thickness (mm)	Power (W)
Be	0.5	300

IN-BEAM TESTS

BEAM-TIME REQUEST

Number of UT's required for beam tuning (including production of radioactive beams in LISE, contact your scientific coordinator)	**5**
Number of UT's required for planned settings/modifications of the experimental set-up	**0**
Number of UT's requested for performing the experiment (data taking) and in-beam calibrations DURING the experiment	**24**
Number of UT's required for performing in-beam tests BEFORE the experiment	**0**
Total number of UT's (sum of the 4 values above)	**29**

SCHEDULING

Date will experiment be ready to run: **January 2023**

SCIENTIFIC PRODUCTION

Status of previous experiments performed by the spokesperson(s) in the last 3 years at GANIL (or related experiments elsewhere):

E738 and E755 experiments were pereformed in 2018 with the same MUST2@LISE and cryogenic target setup.

Two students (S. Koyama and L. Lalanne) got Phd and the publications of the results have started in this year.

Two papers are to be submitted to PRL for each experiment.

Publications, presentations, and theses completed in the last 3 years from past experiments at GANIL (or related experiments elsewhere):

Publications

L. Lalanne, O. Sorlin, et al., Phys. Rev. C 103, 055809 (2021).

S. Koyama, et al., Nucl. Instr. Meth. A 1010, 165477 (2021).

Theses

S. Koyama, the University of Tokyo (2020)

L. Lalanne, the University Paris-Saclay. (2021)

ADDITIONAL INFORMATION

DATA MANAGEMENT

Data Manager: Koyama Shumpei (GANIL)

Additional Data Manager: Shumpei Koyama (GANIL)

Data preservation:	15 years
Embargo Period:	3 years
Estimation of the volume of data generated	1 To

1 Introduction

The structure of atomic nuclei is relatively well described by the single-particle picture for nuclei having magic proton or/and neutron magic numbers, such as 8, 20, 28, 50, 82, 126. In these nuclei, large energy gaps of several MeV exist between occupied and valence orbitals. In a case of strict magicity, the valence states should not be occupied and valence orbitals should be fully vacant. In reality, the atomic nucleus is a correlated system in which the nucleons' occupancy spreads to the valence orbits as well, leading then a diffuse Fermi surface (see Fig. 1). The study of this diffuseness can, therefore, be considered as a major characterization of magicity. We plan to apply it to the N=40 shell gap in ^{68}Ni, N=40 being part of the HO-like magic numbers as 8 and 20. This investigation of the occupancy of the fpg neutron orbitals has been undertaken in stable Ni isotope from ^{58}Ni to ^{64}Ni. It was shown that the partial filling of the $g_{9/2}$ orbital already starts at ^{62}Ni below N=40 [1].

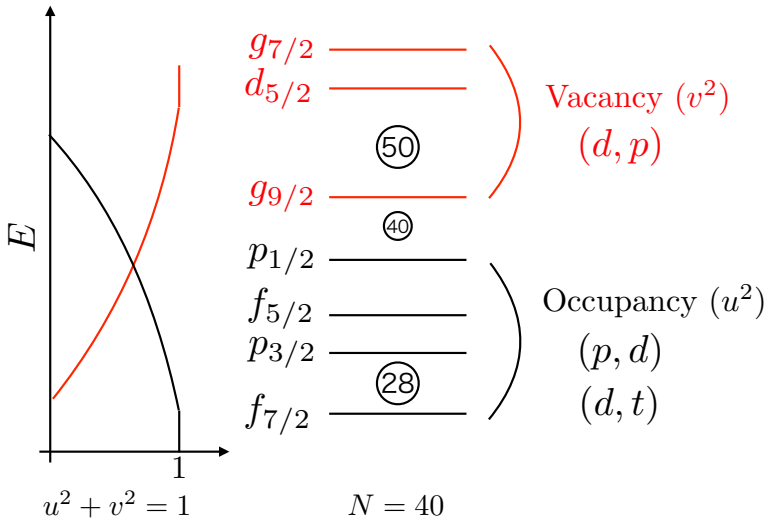

Figure 1: Occupancy and Vacancy for N=40 nuclei.

In nuclei far from the stability line, the disappearance of conventional magic number and the appearance of new magic number, called shell evolution, is observed [4]. To investigate the shell evolution of unstable nuclei, one of the benchmark nuclei is ^{78}Ni, which has the conventional magic numbers of Z=28 and N=50 at far from the stability line. Recently, the 2^+_1 state of ^{78}Ni was measured [5]. Its relatively high-excitation energy of 2.6 MeV reveals that the N=50 magic number is preserved in ^{78}Ni, while the relatively low 2^+_2 state at 2.9 MeV suggests the presence of nearby prolate shape. The 2^+ energy is one piece of information about magicity and neither the amplitude of the N=50 shell gap, nor its evolution by adding neutrons from ^{68}Ni are known. This N=50 shell evolution is, however, very interesting to confirm an early finding of the systematic formation of shell gaps by the action of $3N$ forces [2]. As shown in the middle of Fig. 2, the N=28 shell gap increases when the number of neutrons changes from 20 to 28 in Ca isotope. This effect can be explained when the three-body force is taken into account since this gap is almost constant by considering two-body forces only [6]. This mechanism can also be applied in the case of the N=14 gap in the O isotopic chain [7], as shown in the left part of Fig. 2. Using the same analogy, the N=50 gap between the $d_{5/2}$ and $g_{9/2}$ orbitals is expected to increase when adding the neutron from N=40 to N=50, namely from ^{68}Ni to ^{78}Ni. If a systematic increase of SO-like shell gaps (such as 14, 28 and 50) by about 2.5 MeV is found, this effect must be applied to higher-j orbitals for which such a study is no longer possible as orbits are no longer separated from the others. In order to infer the evolution of the N=50 gap between the $d_{5/2}$ and $g_{9/2}$ neutron orbitals, the starting point is to determine it in ^{68}Ni, at N=40. It can be estimated from the excitation energy $E^+(5/2^+)$ of the $5/2^+$ state(s) in ^{69}Ni, by means of adding a single neutron added in the $d_{5/2}$ orbital of ^{68}Ni, through the (d,p) reaction leading to the $(A+1)$ nucleus ^{69}Ni. The neutron adding spectroscopic factors (C^2S^+) of the $5/2^+$ states will be used to determine the centroid of the $5/2^+$ states, $< E_{d5/2} >$. As for the determination of the $d_{5/2}$ centroid, there is a larger probability that both particle and hole contributions play a role. The hole contribution can be derived from the neutron removal ^{68}Ni$(p,d)^{67}$Ni reaction. The N=50 gap will be derived from $< E_{d5/2} >$- $< E_{g9/2} >$. With this gap value, the neutron-neutron matrix elements derived in this region [2] could be applied to infer the size of the N=50 gap in ^{78}Ni and see if its value is compatible with the one used/obtained in SM calculations for ^{78}Ni. Note that the amplitude of the N=50 shell gap at N=40 is also crucial to account for the onset of collectivity below ^{68}Ni, for which $(j, j+2)$ partners are needed at relatively close energy [8, 9].

Besides the determination of the N=50 shell gap, there is also interesting to study the spin-orbit (SO) splitting of the $2p$, $1f$ (hole) and $1g$ (particle) orbitals in ^{68}Ni. Whenever possible, it will be compared to other Ni isotopes, such as for the $2p$-shells in Fig. 3. This figure shows the scaled SO splitting derived experimentally around closed-shell nuclei, in a broad

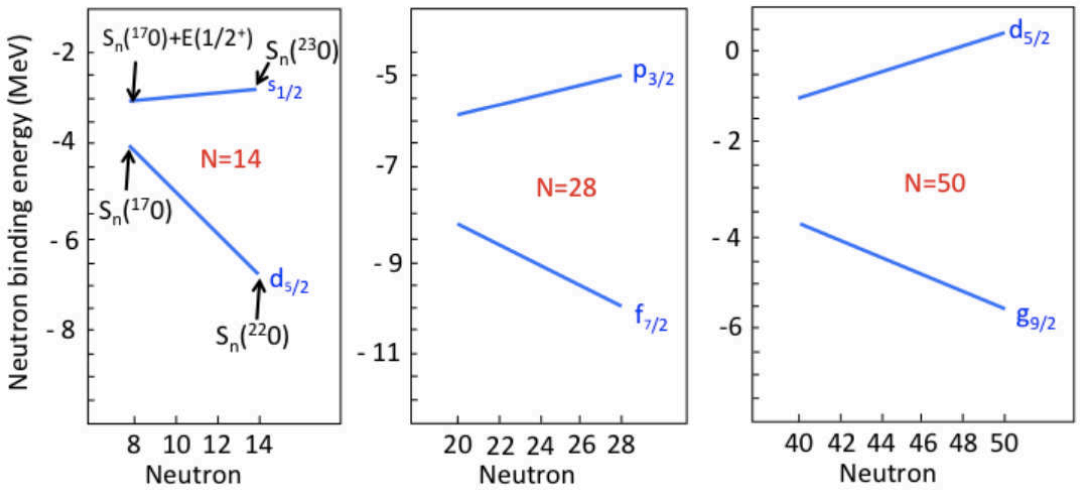

Figure 2: Evolution of neutron binding energies in the O (left), Ca (middle) and Ni (right) isotopic series. The figure is taken from the Fig. 10 of Ref. [2].

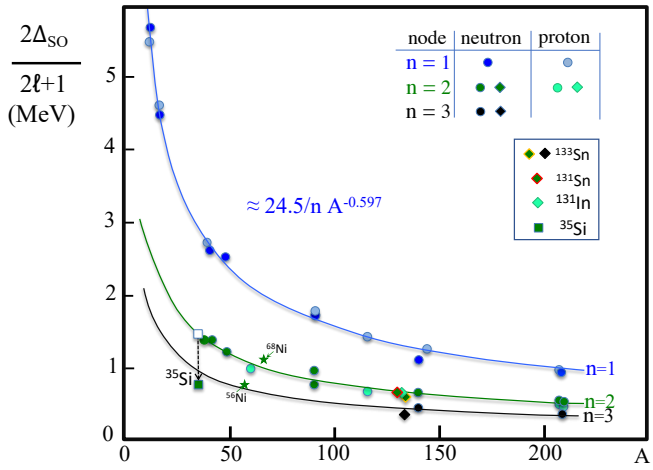

Figure 3: Evolution of SO splitting as a function of A for different value of n, the number of nodes of wave function. Taken from the Fig. 1 of Ref. [3]. The points for ^{68}Ni and ^{56}Ni are added with green star symbols. They are located slightly above and much lower than the expected trend, respectively.

mass region [10]. Though most of the experimental data points nicely follow the empirical curves as a function of A for the radial quantum number $n = 1, 2$ or 3, there is a significant anomaly for $2p_{3/2} - 2p_{1/2}$ SO splitting of ^{35}Si, as discussed in Refs. [11, 3, 12]. The data points for $2p_{3/2} - 2p_{1/2}$ SO splitting, deduced from the $1/2^-$ and $3/2^-$ states identified in ^{57}Ni and ^{67}Ni by means of the ^{56}Ni(d, p) and ^{66}Ni(d, p) reactions, respectively, also display a significant deviation to the global trend that is so far unexplained (read [3] for the case of ^{57}Ni and [13] for ^{67}Ni). An increase of the splitting is observed between them, while a decrease would be expected from the trend. This points to a surprising role of the neutron-neutron interaction when moving from ^{57}Ni to ^{67}Ni, a misidentification of the states, or a missing $1/2^-$ or $3/2^-$ strength in one or the two nuclei. By performing the neutron removal reaction from ^{68}Ni, we can also obtain the spectroscopic information of the $2p$ hole states in ^{68}Ni.

Finally, we could also deduce information on the location of the $g_{7/2}$ particle strength in ^{69}Ni and $f_{7/2}$ hole strength in ^{67}Ni from the neutron adding and removal reactions, respectively. From the above trend, the neutron SO splitting $g_{7/2} - g_{9/2}$ and $f_{5/2} - f_{7/2}$ should be of about 9 and 7 MeV, respectively. The strength is however expected to be very fragmented, in particular for the $g_{7/2}$ orbital.

To summarize, we propose to study the neutron adding and neutron removal reactions from the ^{68}Ni nucleus to study the neutron Fermi surface at N=40, the $g_{9/2} - d_{5/2}$ spacing at N=40, the $2p$ SO splitting, as well as the $1g$ and $1f$ SO splittings.

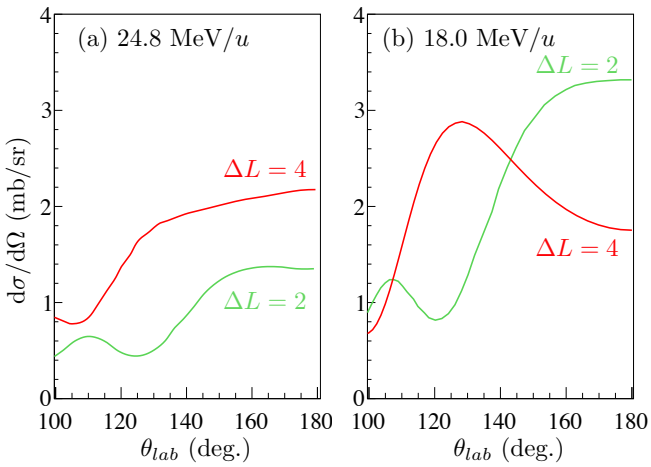

Figure 4: DWBA calculations of the ^{68}Ni$(d,p)^{69}$Ni reaction at 2.8 MeV with $\Delta L = 2$ (green) and 4 (red) for beam energies of (a) 24.8 MeV/u and (b) 18.0 MeV/u.

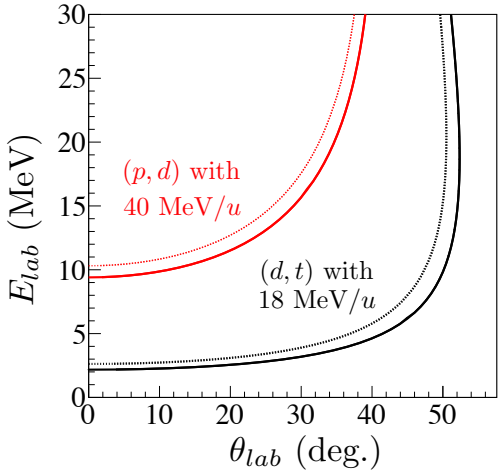

Figure 5: Kinematics of the ^{68}Ni$(d,t)^{67}$Ni (black) and ^{68}Ni$(p,d)^{67}$Ni (red) reactions. Kinematics of ^{67}Ni ground state (solid) and 1.7 MeV excited state (dotted) are shown.

2 Experimental method

The detail for neutron adding and removing reactions for ^{6}8Ni are discussed in this section.

2.1 Neutron adding ^{68}Ni$(d,p)^{69}$Ni reaction

To determine the $2d_{5/2}$ strength, the ^{68}Ni$(d,p)^{69}$Ni reaction is one of the best reactions. By adding a neutron to N=40 "shell closed" ^{68}Ni, we can selectively populate the single particle $2d_{5/2}$ and $1g_{9/2}$ states in ^{69}Ni.

This reaction was once studied at GANIL [14, 15]. Below the excitation energy of 4 MeV, they successfully populated the $2d_{5/2}$ strength at 2.5 MeV in ^{69}Ni. The detailed analysis suggested that the strength at 2.5 MeV was composed of doublet at 2.1 MeV and 2.8 MeV. The angular distribution of the state at 2.1 MeV agrees with the transferred angular momentum (ΔL) of 2, corresponding to a neutron in $2d_{5/2}$, while that at 2.8 MeV agrees with both ΔL =2 and 4. However, the respective contribution of ΔL=2 and 4 was hard to infer as both had similar diffraction pattern of the angular distributions at the beam energy of 24.8 MeV/u, as shown in Fig 4. (a). Moreover, the use of a very thick target prevented an accurate determination of their excitation energies.

In the proposed experiment, we aim at determining the excitation energies of this doublet and confirm the ΔL of each state by the missing mass method. For this purpose, we plan to use a lower beam energy of 18 MeV/u. With this beam energy, the diffraction patterns of the $\Delta L = 2$ and 4 momentum transfer are more different, as shown in Fig. 4 (b). This enables to confirm the ΔL transferred momentum. Furthermore, a higher cross section is expected for $\Delta L = 2$ due to the better momentum matching using a lower beam energy. We also plan to use thinner CD_2 target to separate the two states around 2.5 MeV with better excitation energy resolution and also allow to identify strength coming from the $f_{5/2}$ orbital in the two states tentatively identified at 915 and 1517 keV [16]. To determine the accurate and precise excitation energy, the coincidence measurement of γ-ray is also efficient.

2.2 Neutron removing ^{68}Ni$(d,t)^{67}$Ni and ^{68}Ni$(p,d)^{67}$Ni reactions

To determine the neutron occupancy of ^{68}Ni, we plan to use neutron removing reactions of (d,t) and (p,d) with missing mass and γ-ray spectroscopy. These reactions allow to determine the occupancy of the normally occupied fp-shells, as well as the possibility of a partial occupancy of the valence $1g_{9/2}$ orbital in ^{68}Ni. The spin and parity of the first four states of ^{67}Ni have been assigned in previous measurements, $1/2^-$ for the ground state, 0.7 MeV for the $5/2^-$ state, 1.0 MeV for the $9/2^+$ state with a life time of 13.3 μs and 1.7 MeV for the $3/2^-$ state (see e.g. [13]).

The neutron occupancy of ^{68}Ni was planned to be studied by prompt and delayed γ-ray spectroscopy using the one-neutron knockout reaction [17]. With the method, the spectroscopic factors of each state can in principle be deduced from measured cross sections extracted from the detection of γ-ray deexciting them. The uncertainty of the ground state and excited states from the side-feeding and/or γ-ray emitted after the neutron-emission from the states above the neutron threshold energy of ^{68}Ni can be large. Moreover, this method does not allow to derive occupancy values for isomeric states which do not detect promptly by γ-ray emission. It is also impossible to determine whether the knockout has occurred from the ground or isomeric state. Therefore, no occupancy value can be derived from this study. We will use missing mass method to measure the cross section of directly populated hole states in ^{67}Ni.

In the setup of the ^{68}Ni$(d,p)^{69}$Ni, with a low energy ^{68}Ni beam and thin CD_2 target, we can simultaneously measure the ^{68}Ni$(d,t)^{67}$Ni reaction. In this setup, we can mainly populate the hole states of $2p$-orbital, while the cross section for the g- and f-orbitals are expected to be too small. Therefore, we plan to use the ^{68}Ni$(p,d)^{67}$Ni reaction with a higher energy ^{68}Ni beam of 40 MeV/u and a CH_2 target. The higher recoil energy from the ^{68}Ni$(p,d)^{67}$Ni reaction, as show in Fig. 5, allows to use a thicker CH_2 target with reasonable excitation energy resolution, thus allowing a significant gain in yields. The excited states can be separated in energy by detecting their prompt or delayed γ-rays (for the $9/2^+$ state in ^{67}Ni).

2.3 5^- isomer in ^{68}Ni

Isomeric state at 2.8491 MeV with a life time of 0.86 ms is known in the beam nucleus of ^{68}Ni. In the LISE beam line, the isomer ratio of the beam has been measured to be 31(2)% in Ref. [18]. The effect of the isomer for the missing mass measurement is shortly mentioned.

When incident beam particle is 5^- isomer, the missing mass excitation energy spectra for (d,p) and (p,d) will be shifted by -2.849 MeV (the excitation energy of the isomer). This peak at negative excitation energy was not observed in the previous ^{68}Ni$(d,p)^{69}$Ni measurement [14, 15]. In the neutron knockout reaction of ^{68}Ni, they observed γ-rays from high-spin states, such as $15/2^+$, by most likely knocking out from the 5^- isomer [17]. The strengths of these high-spin states were more fragmented than those of low-lying states, because they have a complex configuration from $1g_{9/2}$ and two holes in different fp-orbits. We thus expect a small contribution of them for the (p,d) and (d,t) reactions as compared to those from the ^{68}Ni ground state.

Table 1: Summary of the secondary beams and targets.

Beam	purity	E_{beam} (MeV/u)	ΔE_{beam} (MeV)	Intensity (pps)	target	thickness (mg/cm^2)	reaction
^{68}Ni	80%	18	$\pm$10	4.0×10^4	CD_2	0.5	(d,p), (d,t)
^{68}Ni	80%	40	$\pm$2	1.6×10^5	CH_2	5	(p,d)

3 Experimental setup

We propose to measure the ^{68}Ni$(d,p)^{69}$Ni and ^{68}Ni$(d,t)^{67}$Ni reactions in inverse kinematics using a ^{68}Ni secondary beam of 18 MeV/u, produced by fragmentation using the LISE spectrometer. We also plan to measure the ^{68}Ni$(p,d)^{67}$Ni reaction at an energy of 40 MeV/u for a complementary measurement. The differences of the two setups (beam energy, intensity and target) are summarized in Tab. 1.

The ^{68}Ni secondary beam at 40 MeV/u will be produced from a ^{70}Zn primary beam of 62 MeV/u with a 500-μm-thick Be primary target titled 20 degrees and a 500-μm-thick Be wedge placed at the intermediate focal plane of LISE. For the 18 MeV/u beam, an additional 700-μm-thick Be degrader is placed in D4 to slow down the beam to the requested energy value. The thickness of the secondary target will be 0.5 mg/cm^2 for CD_2 and 5 mg/cm^2 for CH_2, respectively, optimized in terms of the excitation energy resolution and yields.

We will determine the velocity of each incoming ion with an accuracy of 0.12% by measuring their time of flight (TOF) between the D4 and D6 rooms, separated by a distance of about 27 meters. One CATS detector will be placed in D4, while two more are placed upstream of the secondary target. Each detector has a time resolution of about 300 ps. The reconstructed beam position on target incident is also measured by this latter pair of CATS detectors. Particle identification (PID) of the secondary beam will be performed by this TOF measurement and the energy loss of the ions in an ionization chamber placed in D6.

For the detection of transfer-like products, we will use the MUGAST@LISE setup. Five trapezoidal DSSDs (GRIT) will be placed at backward angles from $110^\circ - 170^\circ$ with an acceptance of 60%. These detectors are used for the (d,p) reaction. In addition, four MUST2 telescopes are placed in the forward angle from $5^\circ - 40^\circ$, with an maximum acceptance of 80%. These detectors are used for the (d,t) and (p,d) reactions. Surrounding the target and recoil particle detectors, the EXOGAM2 detectors are placed for the prompt γ-ray detection.

The Zero Degree Detection system (ZDD) will be placed at the end of the beam line. The ZDD system is composed of a pair of drift chambers, 10 titled foils ionizing chambers and plastic scintillator. The PID in the ionizing chamber and the TOF between CATS and the plastic scintillator allow to clean up the missing mass spectra by removing the reactions from carbon in the CD_2 and CH_2 targets, which lead to quasi-fusion events having heavier mass and longer TOF values. Kinematic correlation between the recoil particle and ejectile measured by the drift chambers will also be used to clean up the spectra by selecting events with the expected two-body kinematics pattern. A clover Ge detector will be placed at the rear of the plastic scintillator of the ZDD in order to determine isomeric contents of the ^{68}Ni beam and of the $9/2^+$ state in ^{67}Ni produced by the (p,d) reaction.

With this setup, the estimated excitation energy resolutions (r.m.s.), obtained by a Monte Carlo simulation using NPTool [19], are 0.14 MeV for (d,p), 0.18 MeV for (d,t) and 0.25 MeV for (p,d). The expected spectra and the kinematics curves are shown in Figs. 6 and 5 with estimated yields below.

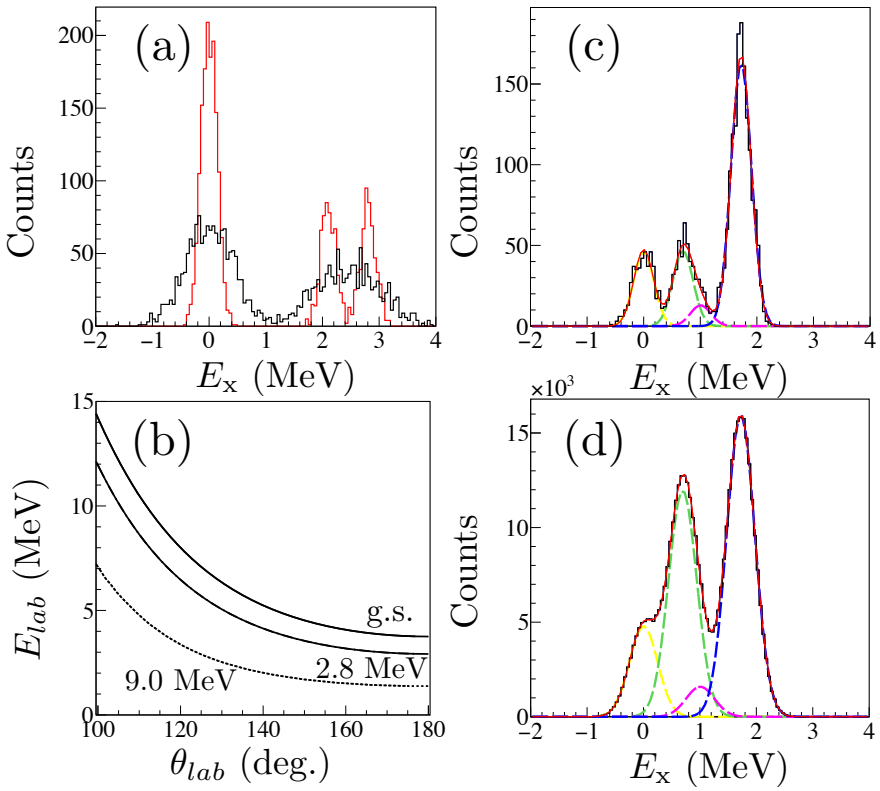

Figure 6: Expected missing mass spectra for each reaction. (a)^{68}Ni$(d,p)^{69}$Ni with the current setup (red) and previous setup [14, 15] (black). (b) Kinematics curves of the ^{68}Ni$(d,p)^{69}$Ni reaction. Expected spectra of (c) ^{68}Ni$(d,t)^{67}$Ni and (d) ^{68}Ni$(p,d)^{67}$Ni. For (c) and (d), the peaks correspond to g.s. (yellow), $5/2^-$ at 0.7 MeV (green), $9/2^+$ at 1.0 MeV (magenta) and $3/2^-$ at 1.7 MeV (blue).

3.1 Yields estimations and beam-time request

The expected yield for each study is estimated by considering the beam intensity, target thickness, acceptance of the detectors, reaction kinematics, the differential cross section deduced from DWBA calculations and the quenching factor of about 0.66 obtained when comparing experimental and theoretical cross sections. The summary of yields is shown in Tab. 2. For the (d,p) reaction, the following values are used;

- Beam intensity of ^{68}Ni : 4×10^4 x 0.8 (purity) x 0.7 (isomer) counts/s
- Target thickness : 0.52 mg/cm^2 or 3.8×10^{-8} atom/mb (deuteron)
- Acceptance (GRIT) : 0.6
- Cross section $110° - 160°$: 6.7 mb ($d_{5/2}$), 8.8 mb ($g_9/2$) by DWBA calculation
- Quenching factor : 0.66
- Beam time request : 15 UTs or 5 days(60×60×24×5 s).

By multiplying these values, we obtain 977 counts for $d_{5/2}$ and 1282 counts for $g_{9/2}$, assuming full C^2S=1 for each orbital. If both of the doublet states around 2.5 MeV are $5/2^+$ with C^2S=0.5, one of the states has the yield of 488 counts for 15 UTs (5days).

For the (d,t) reaction, the yields for 4 low-lying states are estimated in the same manner but C^2S for each states are assumed to be 1.3 ($p_{1/2}$), 5.7 ($f_{5/2}$), 1 ($g_{9/2}$) and 4 ($p_{3/2}$). This means about 10% occupancy for the valence $g_{9/2}$ orbital in the ^{68}Ni g.s. The cross section is summed from 5° to 20° in center of mass angle. The efficiency of EXOGAM2 (around the target) for the $5/2^-$ state(s) and of the clover Ge (at the rear of the plastic of implantation) for $9/2^+$ are estimated to 10% and 5%, respectively. The expected yields obtained from (d,t) are weak for orbitals with large L-value, especially for the $9/2^+$ state.

Table 2: Summary of the expected yields. All γ decays are assumed to proceed directly to the g.s.

Nucleus	reaction	E_x (MeV)	J^π	σ_{DWBA} (mb)	C^2S	missing mass yield	γ eff. (%)	γ coin. yeild
^{69}Ni	(d,p)	0.0	$9/2^+$	8.8	1.0	1282	-	-
		2.1	$5/2^+$	6.7	0.5	488	5	24
		2.7	$5/2^+$	6.7	0.5	488	5	24
^{67}Ni	(d,t)	0.0	$1/2^-$	0.9	1.3	430	-	-
		0.7	$5/2^-$	0.4	5.7	418	10	42
		1.0	$9/2^+$	0.3	1.0	110	5	6
		1.7	$3/2^-$	1.0	4.0	1417	7	103
^{67}Ni	(p,d)	0.0	$1/2^-$	5.6	1.3	32311	-	-
		0.7	$5/2^-$	2.9	5.7	73367	10	7337
		1.0	$9/2^+$	2.1	1.0	9320	5	466
		1.7	$3/2^-$	5.4	4.0	95869	7	6711

For the (p,d) reaction, 8 UTs of beam time are requested to obtain about the same yield of the $d_{5/2}$ state by (d,p) for $g_{9/2}$ strength using the delayed γ-ray coincidence. In the (p,d) reaction, we expect about 100 times more yield then the (d,t) reaction due to the high beam rate ($\times$4), thicker target thickness ($\times$10) and better momentum matching and angular coverage ($\times$6) even with half beam time. The cross section is summed from 5° to 40° in center of mass angle due to the kinematics of the (p,d) reaction shown in Fig. 5. As a result, we expect 466 counts with delayed γ-ray coincidences for the $9/2^+$ state in 8 UTs of measurement.

We request 1 UT for the measurement of the 5^- dependence with the momentum selection of the fragments. In summary, a total, 15 + 8 + 1 = 24 UTs are requested, without the beam tuning.

References

[1] J.P. Schiffer *et al.*, Phys. Rev. Lett. **108**, 022501 (2012).

[2] O. Sorlin and M.G. Porquet, Phys. Scr. **T152**, 014003 (2013).

[3] O. Sorlin, F. de Oliveira Santos and J. Ebran, Phys. Lett. B **809**, 135740 (2020).

[4] O. Sorlin and M.G. Porquet, Prog. Part. Nucl. Phys. **61**, 602–673 (2008).

[5] R. Taniuchi *et al.*, Nature **569**, 53–58 (2019).

[6] J.D. Holt *et al.*, J. Phys. G: Nucl. Part. Phys. **39**, 085111 (2012).

[7] T. Otsuka *et al.*, Phys. Rev. Lett. **105**, 032501 (2010).

[8] O. Sorlin *et al.*, Eur. Phys. J A **16**, 55–61 (2003).

[9] S.M. Lenzi *et al.*, Phys. Rev. C **82**, 054301 (2010).

[10] G. Mairle, Phys. Lett. B **304**, 39–44 (1993).

[11] G. Burgunder *et al.*, Phys. Rev. Lett. **112**, 042502 (2014).

[12] T. Duguet *et al.*, Phys. Rev. C **95**, 034319 (2017).

[13] J. Diriken *et al.*, Phys. Rev. C **91**, 054321 (2015).

[14] M. Moukaddam *et al.*, Acta Phys. Pol. B **42**, 541 (2011).

[15] M. Moukaddam, Phd Thesis (2011).

[16] W.F. Mueller *et al.*, Phys. Rev. Lett. **83**, 3613–3616 (1999).

[17] F. Recchia *et al.*, Phys. Rev. C **94**, 054324 (2016).

[18] S. Calinescu *et al.*, Phys. Rev. C **104**, 034318 (2021).

[19] A. Matta *et al.*, J. Phys. G: Nucl. Part. Phys. **43**, 045113 (2016).